Solution Structure of Marinostatin, a Natural Ester-Linked Protein Protease Inhibitor‡

Kenji Kanaori,§ Kaeko Kamei,*,§ Mai Taniguchi,§ Takao Koyama,§ Tomoharu Yasui,§ Ryo Takano,§ Chiaki Imada,|| Kunihiko Tajima,§ and Saburo Hara§

Department of Applied Biology, Kyoto Institute of Technology, Matsugasaki, Sakyo-ku, Kyoto 606-8585, and Department of Food Science and Technology, Tokyo University of Fisheries, Minato-ku, Konan 4-5-7, Tokyo 108-8477, Japan

Received September 11, 2004; Revised Manuscript Received December 8, 2004

ABSTRACT: Marinostatin is a unique protein protease inhibitor containing two ester linkages. We have purified a 12-residue marinostatin [MST(1−12), ^{1}FATMRYPSDSDE^{12}] and determined the residues involved in the formation of the ester linkages and the solution structure by ^{1}H NMR spectroscopy and restrained molecular dynamics calculation. The two ester linkages of MST(1−12) are formed between hydroxyl and carboxyl groups, Thr^{3}−Asp^{9} and Ser^{8}−Asp^{11}, indicating that MST(1−12) has two cyclic regions which are fused at the residues of Ser^{8} and Asp^{9}. A strong NOE cross-peak between Tyr^{6} H_{α} and Pro^{7} H_{α} was observed, indicating that the Pro^{7} residue takes a *cis*-conformation. Well-converged structures and hydrogen−deuterium experiments of MST(1−12) showed that the backbone NH proton of the P1′ residue, Arg^{5}, is hydrogen-bonded to the carbonyl oxygen of the ester linkage between Thr^{3} and Asp^{9}. To reveal the significance of the ester linkages, a marinostatin analogue, MST-2SS (^{1}FACMRYPCCSCE^{12}) with two disulfide bridges of Cys^{3}−Cys^{9} and Cys^{8}−Cys^{11}, was also synthesized. The inhibitory activity of MST-2SS was as strong as that of MST(1−12), and the Pro^{7} residue of MST-2SS also takes a *cis*-conformation. However, the exchange rate of the Arg^{5} NH proton of MST-2SS was about 100 times faster than that of MST(1−12), and the structure calculation of MST-2SS was not converged on account of the small number of NOEs, indicating that MST-2SS takes a more flexible structure. The hydrogen acceptability of the ester linkage formed by the P2 position residue, Thr^{3}, is crucial for suppressing the fluctuation of the reactive site and sustaining the inhibitory activity, which enables marinostatin to be one of the smallest protease inhibitors in nature.

Disulfide bridges form as a protein folds to its native conformation; they function to stabilize its three-dimensional structure. Regardless of various functional groups of 20 standard amino acids, almost all secreted proteins choose disulfide bridges as a stabilizing tool. Is there any protein which chooses other covalent linkages between the functional groups of amino acids, instead of a disulfide linkage, for stabilizing itself? One decade ago, we suggested the existence of a natural ester-linked protein whose name is marinostatin (MST),[1] produced by a marine microorganism, *Alteromonas* sp. B-10-31. MST is a protein protease inhibitor against subtilisin, chymotrypsin, and elastase at an enzyme:inhibitor ratio of 1:1, but not trypsin (*1*−*4*). The biological function is retained by a short fragment comprising 12 amino acid residues, FATMRYPSDSDE, and its scissile peptide bond is determined in the position between Met and Arg (*3*). We reported that the inhibitory activity of MST disappeared in alkaline conditions, and that the molecular weight of MST-(1−12) was increased by two H_2O molecules after the alkaline treatment. Therefore, MST was considered to possess two internal ester linkages between the hydroxyl (Ser or Thr) and carboxyl (Asp or Glu) residues.

All the protein inhibitors prevent access of substrates to the catalytic sites of proteases through steric hindrance (*5*−*7*). The majority of the protein inhibitors known and characterized so far are directed toward serine proteases. Most serine protease inhibitors achieve their inhibitory activity by binding of their peptide segment directly to the catalytic site in a substrate-like manner. The serine protease inhibitors take a compact shape with an exposed flexible binding loop and a hydrophobic core which is mostly rigid due to the cross-connecting disulfide bridges. In binding of the inhibitors to the protease, intra- and intermolecular interactions of the inhibitor's primary binding segment with the inhibitor's core and with the enzyme's binding site mutually stabilize each other and are so tight that decomposition of the inhibitor rarely occurs. The rigid hydrophobic core with disulfide bridges is considered to be indispensable for the canonical inhibitory manner. Taking into account that serine protease inhibitors known so far consist of between 14 and around 190 amino acid residues (*7*−*10*), the number of amino acids required for the inhibitory activity of MST

‡ Atomic coordinates for MST(1−12) have been deposited in the Protein Data Bank (accession code 1IXU).

* To whom correspondence should be addressed. Phone: +81-(75)-724-7553. Fax: +81-(75)-724-7532. E-mail: kame@kit.ac.jp.

§ Kyoto Institute of Technology.

|| Tokyo University of Fisheries.

[1] Abbreviations: MST, marinostatin; MST(1−12), a 12-residue marinostatin; MST-2SS, a marinostatin disulfide analogue; CD, circular dichroism; 1D, one-dimensional; 2D, two-dimensional; DQF-COSY, double-quantum-filtered correlated spectroscopy; TOCSY, total correlation spectroscopy; NOESY, nuclear Overhauser enhancement spectroscopy.

10.1021/bi048034x CCC: $30.25
Published on Web 01/29/2005

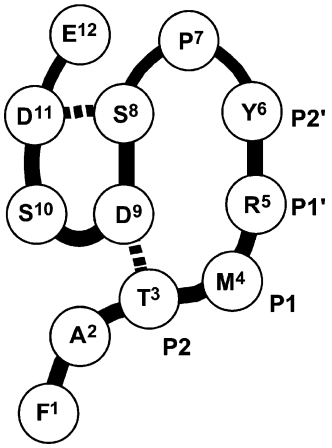

FIGURE 1: Schematic drawings of MST(1−12). Dashed lines indicate ester linkages.

is likely too small to form a rigid hydrophobic core, implying that the characteristic ester linkages should play an essential role in making MST such a small protein protease inhibitor.

In this study, we have purified a 12-residue MST [MST-(1−12), ^{1}FATMRYPSDSDE^{12}] as previously reported (*1*), and determined the residues involved in the formation of the ester linkages (Thr^{3}−Asp^{9} and Ser^{8}−Asp^{11}) (Figure 1), and the solution structure by ^{1}H NMR spectroscopy. To our knowledge, this work is the first structural study on a natural protein which has two ester linkages, and one of the smallest protease inhibitors working in a canonical inhibitory manner. Furthermore, we have selectively synthesized a marinostatin analogue, MST-2SS (^{1}FACMRYPCCSCE^{12}) with two disulfide bridges of Cys^{3}−Cys^{9} and Cys^{8}−Cys^{11}, and have discussed inhibitory activity and structure as compared to those of MST(1−12) to reveal the significance of the ester linkages.

MATERIALS AND METHODS

Sample Preparation and Inhibitor Activity Measurements. MST(1−12) was purified according to the modified method of a previous report (*1*). The strain *Alteromonas* sp. was cultivated in artificial seawater, pH 6.6, containing 0.48% (w/v) sodium glutamate, 0.12% (w/v) casamino acid, 0.2% (w/v) glucose, and 0.01% *N*-acetylglucosamine at 24 °C for 96 h under shaking at 100 rpm. By adding Diaion HP20 resin (Nippon Rensui Co., Japan) to the culture medium, MSTs were adsorbed to the resin, and then eluted with 80% methanol to obtain crude MSTs. The crude sample was further purified by reversed-phase chromatography on YFLC gel C18 (15 μm) followed by gel filtration on cellulofine GCL-25m (Seikagaku Corp., Japan), and repetitive ion-exchange chromatographies by CM-cellulofine (Seikagaku) and HiLoad S (Pharmacia). Finally, MST(1−12) was purified by reversed-phase HPLC using Inertsil ODS-3 (GL Science, Japan). The inhibitory activity against subtilisin BPN′ was measured in phosphate buffer, pH 7.0, at 30 °C using Suc-Ala-Ala-Pro-Phe-MCA as a substrate. The K_i value was calculated as described by Green and Work (*11*). The amino acid analysis was performed with a Hitachi L-8500 amino acid analyzer after 24 h of hydrolysis with 6 N HCl. The amino acid sequence was determined by an automated gas-phase sequencer, Shimadzu PPSQ-10, and the molecular weight was confirmed by a MALDI-TOF mass spectrometer, Bruker-Daltonik, Reflex III. The amino acid analysis showed that the chemical composition of MST-(1−12) was $C_{60}H_{87}N_{15}O_{23}S$, and the mass spectral analysis gave a parent peak corresponding to $C_{60}H_{87}N_{15}O_{23}S-2H_2O$. After the alkaline treatment, the molecular weight of MST-(1−12) was increased by 36.0, and the inhibitory activity was completely lost as previously reported (*2*, *3*).

Synthesis of MST-2SS. MST-2SS was synthesized by the Fmoc method on an automatic solid-phase peptide synthesizer, PSSM-8 (Shimadzu, Japan). To form the disulfide linkages selectively, the side chain groups of Cys at positions 3 and 9 were protected with trityl groups, and those at positions 8 and 11 with acetamidomethyl groups. After synthesis, the peptide was cleaved from the resin and deblocked by 82% trifluoroacetic acid containing 5% H_2O, 5% thioanisole, 3% 1,2-ethanedithiole, 2% ethyl methyl sulfide, and 3% phenol for 8 h. Under these conditions, all the protecting groups other than the acetamidomethyl groups were removed. Then, the peptide was dissolved at a concentration of 0.1 mg mL^{-1} in 30 mM ammonium bicarbonate (pH 8.0), and kept under stirring at room temperature for 3 days. Thus, the peptide was oxidized by O_2 in air to form a disulfide linkage of Cys^{3}−Cys^{9}. After lyophilizing, the peptide was dissolved with 80% methanol/20% H_2O (the peptide concentration was 1 mg mL^{-1}). To remove the acetamidomethyl groups and form the disulfide linkage between Cys^{8} and Cys^{11}, the solution was dropped into a mixture of methanol (1.0 mL/mg of peptide), 6 N HCl (0.4 mL/mg of peptide), and iodine solution (1.5 mL/mg of peptide) (76 mg of iodine/15 mL of methanol) under vigorous stirring on ice for 10 min, followed by further stirring for 10 min. For neutralization of iodine, ascorbic acid solution (4 mg mL^{-1}) was added to the mixture until it became colorless. The obtained MST-2SS was purified by repetitive reversed-phase chromatography with Develosil-ODS (Nomura Chemicals, Japan) and Inertsil ODS-3 (GL Science) using HPLC. The synthesis and purity of the inhibitor were confirmed by amino acid and sequence analyses and mass spectrometry as well as MST-(1−12). The molecular weight was determined to be 1408.7.

NMR Spectroscopy. For the acquisition of NMR spectra, a 1.0−2.0 mM concentration of the peptide sample was dissolved in 90% H_2O/10% D_2O or 100% D_2O solution at pH 3.0 (meter reading of the glass electrode without correction). All ^{1}H NMR spectra were recorded on a Bruker ARX-500 spectrometer at 5 and 10 °C. 2D DQF-COSY (*12*) and TOCSY (*13*) spectra were acquired to identify spin systems through a chemical bond, and 2D NOESY (*14*) spectra were recorded with mixing times of 80, 150, 350, and 500 ms. The NOESY spectra with the longer mixing times of 350 and 500 ms were only used for signal assignment. 3-(Trimethylsilyl)propionate-d_4 was used as an internal standard of chemical shift. Measurements of ^{3}J coupling constants were obtained from a 1D spectrum. The exchange of amide protons with deuterium was studied at 5 °C on the peptide samples lyophilized from H_2O at pH 3.0 and dissolved in pure D_2O.

Structure Calculations. Molecular modeling and calculations were carried out using the NMR refine module of InsightII version 2.3.0 and Discover version 2.9.5 (Biosym Inc.) on a Silicon Graphic IRIS Indigo^{2} computer. The AMBER force field was employed in all calculations. Distance constraints used as input for the distance geometry

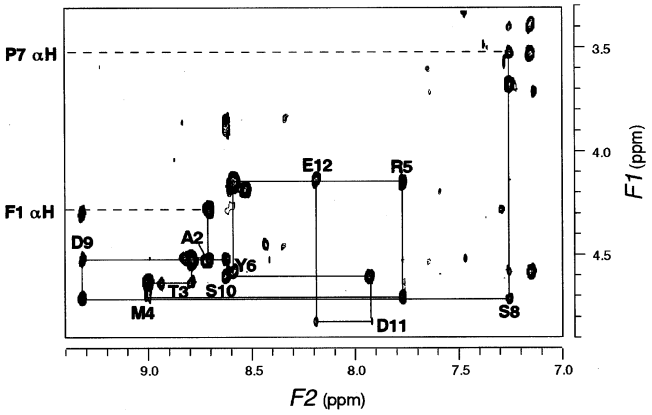

FIGURE 2: NH−αH region of the NOESY spectrum (mixing time 350 ms) of MST(1−12). The $d_{\alpha N}(i,i+1)$ connectivities are indicated by solid lines, and the peaks are labeled by residue type and number at the position of the intraresidual NH−αH cross-peaks.

calculations were determined by integrating NOE cross-peaks derived from the NOESY spectra with mixing times of 80 and 150 ms by using NMR analysis software FELIX and the NMR model module. The NOE-derived distances were calculated by the isolated spin-pair approximation relationship $r_{ij} = r_{ref}(NOE_{ref}/NOE_{ij})^{1/6}$, where r_{ij} and NOE_{ij} are the unknown distance and measured NOE volume between protons i and j, and r_{ref} and NOE_{ref} represent the reference distance (1.8 Å for methylene protons) and the relevant NOE volume. The constraints were classified into four categories (*15*−*18*): strong (<2.5 Å), medium (2.5−3.0 Å), weak (3.0−4.0 Å), very weak (>4.0 Å). For restrained molecular dynamics calculations, the upper bounds were defined as strong (+0.3 Å), medium (+0.3 Å), weak (+0.5 Å), and very weak (+1.0 Å). For ^3J coupling constraints, an error of 1 Hz was employed. Fifty calculations were carried out by using the simulated annealing protocol of the NMR refine module. Restrained energy minimization (rEM) and restrained molecular dynamics (rMD) calculations of 15 ps (time steps of 1.0 fs) at 1000 K were first carried out to search conformational space for structures consistent with the constraints. Then, the temperature was gradually reduced from 1000 to 300 K in a cooling step of 6 ps with increasing nonbonded term, and final rMD calculations of 4 ps at 300 K and rEM calculations were carried out.

RESULTS AND DISCUSSION

Determination of Ester Linkages. The full resonance assignment of the NMR signals of MST(1−12) was performed using the sequential assignment procedure (*19*). The identification of amino acid spin systems was first established by means of direct and relayed through-bond connectivities (DQF-COSY and TOCSY), followed by sequential resonance assignments using through-space NOE connectivities (Figure 2). The resonance assignment of MST(1−12) is summarized in Table S1 in the Supporting Information. For determining the position of the two ester linkages, it should be noted that the formation of the ester linkage causes the downfield shift for Ser or Thr H_β protons by the induced effect of the substitution of a hydroxyl group (−OH) to an ester group (−O−CO−) (*20*). The Thr^3 H_β proton and one of the Ser^8 H_β protons were observed at 5.57 and 4.97 ppm, respectively, which are extraordinarily larger values than the standard ones reported for a random coiled structure (*21*). In addition to

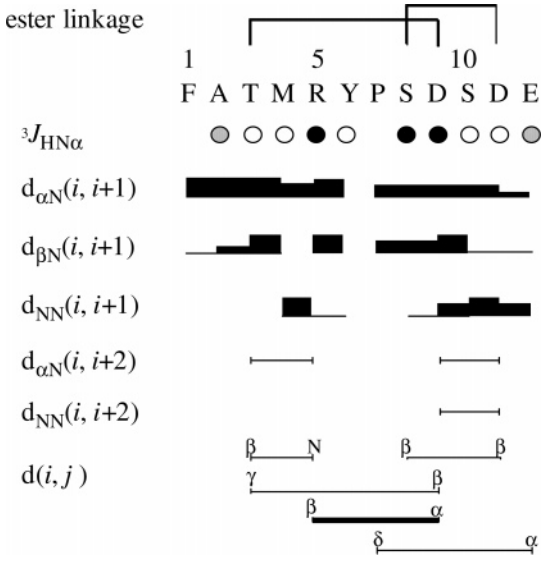

FIGURE 3: Amino acid sequence of MST(1−12) together with a summary of the NOE connectivities of the neighboring residues. The following symbols are used: open circles indicate that $^3J_{HN\alpha}$ > 8.0 Hz, filled circles that $^3J_{HN\alpha}$ < 6.0 Hz, and shaded circles that $^3J_{HN\alpha}$ is between 6.0 and 8.0 Hz. The terms $d_{NN}(i,i+1)$, $d_{\alpha N}(i,i+1)$, and $d_{\beta N}(i,i+1)$ represent the sequential backbone connectivities. The intensities of the observed NOEs are represented by the thickness of the lines.

these prominent downfield shifts of the H_β protons, NOE cross-peaks between Thr^3 $_\gamma CH_3$ and Asp^9 H_β and Ser^8 H_β and Asp^{11} H_β were observed. Thus, we concluded that the two ester linkages of MST(1−12) are formed between hydroxyl and carboxyl groups, Thr^3−Asp^9 and Ser^8−Asp^{11}, indicating that MST(1−12) has two cyclic regions which are fused at the residues of Ser^8 and Asp^9 (Figure 1). To confirm the positions of the ester linkage, we measured the inhibitory activity of MST-2SS. The K_i value of MST-2SS against subtilisin BPN′ was determined to be 3.4×10^{-9} M, which was almost identical to that of MST(1−12) (1.5×10^{-9} M). The near coincidence of the two K_i values justifies the conclusion that the ester linkages of MST exist in the positions of Thr^3−Asp^9 and Ser^8−Asp^{11}. The P2 residue, Thr^3, is connected to the C-terminal cyclic regions by the ester linkage. In general, a P3 position of canonical serine protease inhibitors against subtilisin is commonly disulfide-connected to the hydrophobic core to stabilize a binding loop (*7*). The connection by the ester linkage between the P2 residue and the rest of MST(1−12) indicates that MST, although an ester-linked inhibitor, possesses a common structural feature to stabilize the reactive site.

Description of the Structure of MST(1−12). For the N-terminal cyclic region, a strong NOE cross-peak between Tyr^6 H_α and Pro^7 H_α was observed, indicating that the Pro^7 residue takes a *cis*-conformation. The *cis*-conformation is supported by a prominent upfield shift of the Pro^7 H_α proton (3.53 ppm), because a H_α proton of a *cis*-proline residue is likely shifted more upfield than that of a *trans*-proline (*21*, *22*). The requirement of *cis*-Pro at the P3′ position was reported for a small Bowman−Birk inhibitor (*23*). NOE cross-peaks were observed between side chains of Tyr^6 and Pro^7 with an additional NOE between Tyr^6 H_α and Ser^8 NH, suggesting a well-defined turn in the residue range of Tyr^6-Pro^7-Ser^8. The compact structure in the N-terminal cyclic region was also indicated by NOE cross-peaks between

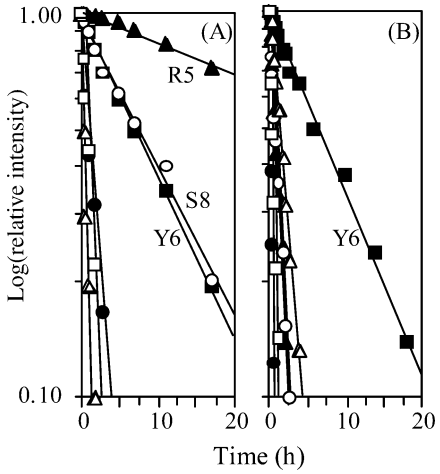

FIGURE 4: Hydrogen−deuterium exchange profile of the amide protons of (A) MST(1−12) and (B) MST-2SS as a function of time after the dissolution of the peptide in D_2O: residues 4 (filled circle), 5 (filled triangle), 6 (filled square), 8 (open circle), 11 (open triangle), and 12 (open square).

Arg^5 H_β/H_ϵ and Asp^9 H_α (Figure 3). This NOE means that the H_α proton of Asp^9 whose side chain is involved in the ester linkage is directed to the inside of the N-terminal cyclic region, whereas that of Arg^5 is directed outside. For the C-terminal cyclic region formed by the Ser^8−Asp^{11} ester linkage with the C-terminal residue, Glu^{12}, the medium and strong NOE connectivities of $d_{NN}(i,i+1)$ were observed in the residue range from Asp^9 to Glu^{12}, and weak NOE cross-peaks of $d_{NN}(i,i+2)$ and $d_{\alpha N}(i,i+2)$ between Asp^9 and Ser^{11}. In addition, NOE cross-peaks between Pro^7 H_δ and Glu^{12} H_α were observed, indicating that the residues in the C-terminal cyclic region take a consecutive turn and that the C-terminal residue is returned back to the N-terminal cyclic region and involved in the well-ordered structure.

Hydrogen−deuterium experiments of MST(1−12) showed that the backbone NH protons of Arg^5, Tyr^6, and Ser^8 were slowly exchanged (Figure 4): The exchange rate of Arg^5 was the slowest one, 3×10^{-4} min^{-1}, and those of Tyr^6 and Ser^8 were both 2×10^{-3} min^{-1}. Those exchange rates were significantly slower than those of a random coiled peptide (*24*). The structure calculation of MST(1−12) using NOE and *J* coupling constraints alone showed that a carbonyl oxygen of the ester linkage between Thr^3 and Asp^9 is suitable for a hydrogen bond acceptor of Arg^5 NH. MST-2SS, an MST analogue with two disulfide bridges, showed that the hydrogen−deuterium exchange rate of the Arg^5 NH proton was about 100 times that of MST(1−12). Therefore, we concluded that the slow exchange rate of Arg^5 NH of MST-(1−12) arises from the hydrogen bond to the ester linkage.

The final structure calculation of MST(1−12) was carried out by employing one hydrogen bond constraint between Arg^5 NH and the ester C═O of Thr^3−Asp^9 besides the NOE and *J* coupling constraints. Twenty-three final structures which showed low total and NOE energy (Figure S1 in the Supporting Information) were chosen for following structure analysis. Figure 5 shows a superposition overlay of the backbone atoms of residues from 3 to 12, and the statistics for the final structures are listed in Table 1. The well-converged structures in the N-terminal cyclic region consisted of the rigid turn of Tyr^6-Pro^7-Ser^8 and of the ester linkage between Thr^3 and Asp^9 with hydrogen bonding to the backbone Arg^5 NH of the P1′ residue. The C-terminal cyclic region was also converged, although the direction of the other ester group of Ser^8−Asp^{11} was dispersed, and the mutual location between the N- and C-cyclic regions was defined. The stabilization of the binding loop by hydrogen bonds or electrostatic interaction from the protein scaffold has been observed for most protease inhibitors (*7*, *25*, *26*). As this point illustrates, MST like other canonical protease inhibitors possesses common stabilization mechanisms for the reactive site by using the characteristics of the ester linkage.

Structure of MST-2SS. To investigate an effect of the ester linkage on the structure, the NMR spectra of MST-2SS were

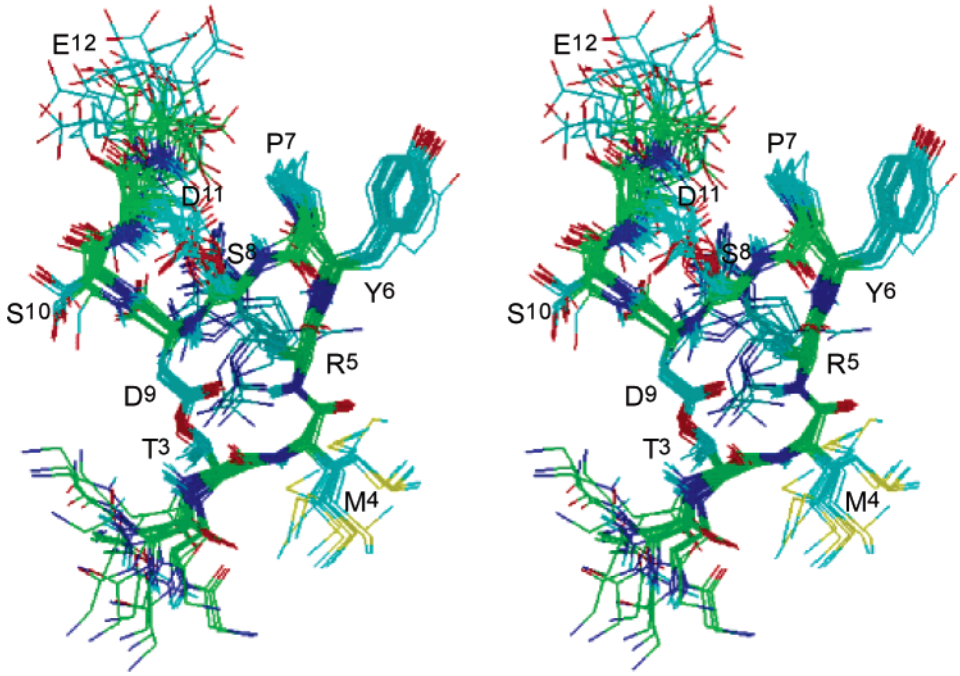

FIGURE 5: Stereoview of the 23 refined structures of MST(1−12) superimposed over the backbone atoms of residues 3−12. The backbone of residues 1−12 is shown with all the side chains except for Phe^1 and Ala^2.

Table 1: Experimental Restraints and Structure Statistics for MST(1−12)

number of analyzed structures	23
number of distance restraints[a]	100 (52)
number of dihedral angle restraints	17
rmsd from experimental distance restraints (Å)	0.008 ± 0.001
number of NOE violations >0.2 Å[b]	3.9 ± 1.2
largest NOE violation (Å)	0.31 ± 0.12
rmsd from experimental dihedral restraints (deg)	1.3 ± 0.2
DISCOVER potential energies[c] (kcal mol^{-1})	
total energy	23.7 ± 5.3
nonbond energy	−15.3 ± 3.9
^3J dihedral forcing potential	0.7 ± 0.4
NOE forcing potential	10.1 ± 2.2
Cartesian coordinate rmsd[d] (Å)	
backbone	0.89 ± 0.30
all heavy atoms	1.85 ± 0.40

[a] The number of distance restraints for MST(1−12) includes one hydrogen-bond restraint. The number in parentheses is that of inter-residue NOEs. [b] None of the structures have distance violations greater than 0.5 Å. [c] The force constants of NOE and ^3J dihedral angle are 20 kcal mol^{-1} A^{-2} and 20 kcal mol^{-1} rad^{-1}, respectively. [d] Rmsd values for MST(1−12) are obtained for residues 3−12.

Table 2: Backbone ϕ and φ Angles (deg) in MST(1−12) Compared with the Corresponding Values in SSI[a] and OMTKY3[b]

	P2 ϕ, φ	P1 ϕ, φ	P1′ ϕ, φ	P2′ ϕ, φ
MST(1∠12)	Thr^3 −61 ± 16, 111 ± 3	Met^4 −87 ± 4, 34 ± 2	Arg^5 −61 ± 4, 177 ± 4	Tyr^6 −80 ± 7, 96 ± 2
SSI	Pro^{72} −66, 149	Met^{73} −81, 64	Val^{74} −95, 157	Tyr^{75} −124, 85
OMTKY3	Thr^{17} −68, 160	Leu^{18} −107, 32	Glu^{19} −74, 159	Tyr^{20} −113, 107

[a] PDB accession code 3SSI (*28*). [b] PDB accession code 1CHO (*29*).

analyzed by the same procedure as those of MST(1−12). A strong NOE cross-peak between Tyr^6 H_α and Pro^7 H_α indicative of a *cis*-conformation and NOE cross-peaks between Arg^5 and Cys^9 were observed for MST-2SS as well as MST(1−12). However, the number of NOE cross-peaks observed for MST-2SS was smaller than that for MST-(1−12). No long-range NOEs were observed for the C-terminal region of MST-2SS. Moreover, Arg^5, Tyr^6, and Cys^8 NH signals and Pro^7 H_α signals were broadened by some intermediate conformational exchange, so the $^3J_{HN\alpha}$ coupling constants were not obtained for these residues. Thus, the structural calculation of MST-2SS showed poor convergence between the lowest energy conformations, and the mutual location of the N- and C-cycling regions could not be defined. For MST-2SS, one slowly exchanging amide proton, Tyr^6 NH (2×10^{-3} min^{-1}), was observed (Figure 4B). The coincidence of the exchange rate of Tyr^6 NH between MST-(1−12) and MST-2SS within experimental error means that both the inhibitors take a similar rigid turn structure in the region of Tyr^6-Pro^7-Ser^8. As mentioned above, the Arg^5 NH of MST-2SS exchanged much faster than that of MST-(1−12), and the Cys^8 NH of MST-2SS also exchanged faster, as compared to the corresponding residue (Ser^8) of MST-(1−12). The undefined mutual position between the N- and C-cyclic regions of MST-2SS should cause the fast exchange of the Cys^8 residue, because the amide proton of Ser^8 in MST(1−12) is covered with the C-cyclic region (Figure 5). The existence of the structural difference between MST-2SS and MST(1−12) is also suggested by large chemical shift differences ($|\delta| > 0.2$ ppm) of the corresponding H_α protons for Met^4, Arg^5, Tyr^6, and Cys^9 of MST-2SS (Table S2 in the Supporting Information), and by the $^3J_{HN\alpha}$ coupling constant difference for Met^4 and Tyr^6. Since the H_α chemical shift and $^3J_{HN\alpha}$ are indicative of the secondary structure (*21*), these differences suggest that these two structures are different around the reactive site in the absence of the protease.

Comparison with Other Subtilisin Inhibitors. The comparison between the two inhibitors indicates that the two disulfide linkages could not suppress the structural fluctuation of MST-2SS and that MST-2SS takes a more flexible and less compact conformation than MST(1−12). It was reported that the disappearance of the interaction between the loop and the scaffold results in considerable enhancement of the loop mobility and reduced rigidity of the scaffold (*10*, *27*). The hydrogen bond of the ester linkage to the amide proton of the P1′ residue would be crucial for suppressing the conformational fluctuation of the fused two-cyclic structure

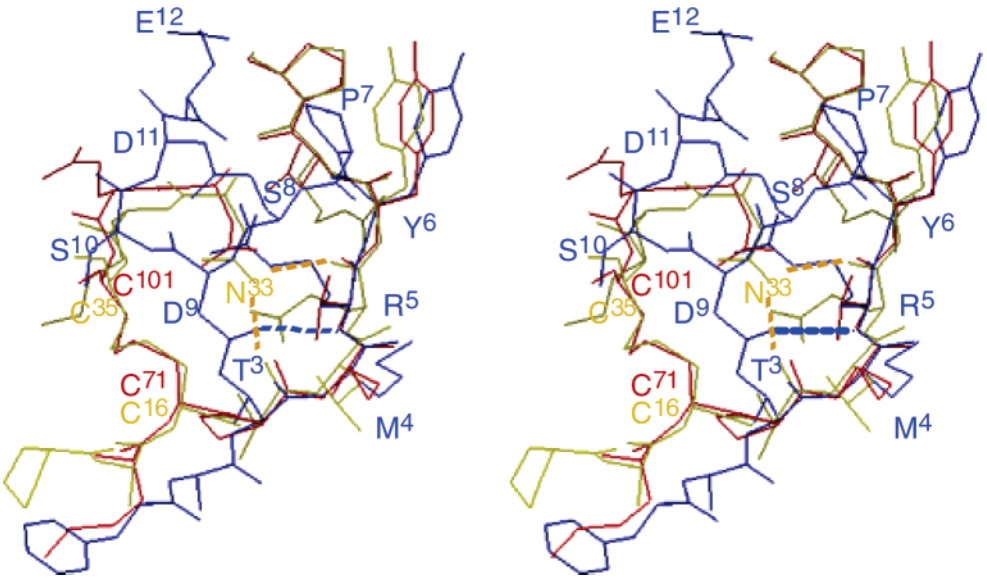

FIGURE 6: Stereoview of MST(1−12) (blue), SSI (red), and OMTKY3 (yellow) superimposed over the α-carbons from P2 to P2′ residues. Broken lines indicate a hydrogen bond (see the text).

of marinostatin, contributing to the duration of the inhibitory activity.

The sequence around the reactive site (P2−P2′) of MST is homologous to those of Kazal and SSI families as shown in Table 2. The amino acids at the P1 (Met) and P2′ (Tyr) positions of MST are identical with those of SSI, and Thr at the P2 site is frequently observed for these families (*7*). The averaged ϕ and φ dihedral angles of P2 to P2′ of MST(1−12) are compared with those of SSI (*28*) and turkey ovomucoid third domain (OMTKY3) (*29*), which have a characteristic canonical extended conformation. The ϕ and φ values of MST(1−12) mainly coincide with the values of those inhibitors, indicating that MST binds to an active pocket of proteases in the same manner as SSI or OMTKY3. It has been pointed out that, in the SSI and Kazal inhibitors, the reactive site loop is tightly held from both sides of the scissile bond by two structural devices (*7, 30*): the β-sheet in the C-terminal side and the disulfide bridge in the N-terminal side. In the case of MST(1−12), the scissile bond of Met^4−Arg^5 is fixed both by the rigid turn of Tyr^6-Pro^7-Ser^8 and by the ester linkage between Thr^3 and Asp^9. However, the structural analysis of MST-2SS demonstrates that the rigid turn and the covalent bond between residues 3 and 9 could not suppress the fluctuation around the reactive site. When the binding loop (P2−P2′) of MST(1−12) is overlaid onto that of SSI or OMTKY3, MST(1−12) fits into a spatial room lying between the binding loop and α-helix of the inhibitors (Figure 6). The Ser^8 and Asp^9 residues of MST(1−12) fill up the middle of the room, and the ester linkage between Thr^3 and Asp^9 is located near the side chain of Asn^{33} of OMTKY3. The amide group of this evolutionally conserved Asn residue is hydrogen-bonded to the main-chain carbonyl oxygens of the P2 and P1′ residues, and plays an important role in fixing the two peptide groups flanking the scissile bond (*29*). Therefore, the ester linkage of Thr^3−Asp^9 by itself possesses two functions that OMTKY3 serves by the disulfide bridge and by the Asn residue. Since the ester linkage is connected to the P2 position and the ester linkage is just hydrogen-bonded to the amide proton of the scissile bond, the ester linkage may suppress fluctuation in the reactive site more efficiently. The dual-functional device, the ester linkage enables MST to be the smallest canonical protease inhibitor in nature, and the structural motif of MST will give us a clue for rational design of various protease inhibitors.

SUPPORTING INFORMATION AVAILABLE

^{1}H NMR assignment of MST(1−12) and MST-2SS (Table S1 and S2) and a plot of the NOE forcing energy against total energy (Figure S1) (PDF). This material is available free of charge via the Internet at http://pubs.acs.org.

REFERENCES

1. Imada, C., Taga, N., and Maeda, M. (1985) Isolation and characterization of marine bacteria producing protease inhibitor, *Bull. Jpn. Soc. Sci. Fish. 51*, 805−810.
2. Imada, C., Hara, S., Maeda, M., and Simidu, U. (1986) Amino acid sequences of Marinostatins C-1 and C-2 from marine *Alteromonas* sp, *Bull. Jpn. Soc. Sci. Fish. 52*, 1455−1459.
3. Takano, R., Imada, C., Kamei, K., and Hara, S. (1991) The reactive site of marinostatin, a proteinase inhibitor from marine *Alteromonas* sp. B-10-31, *J. Biochem. 110*, 856−858.
4. Miyamoto, K., Tsujibo, H., Hikita, Y., Tanaka, K., Miyamoto, S., Hishimoto, M., Imada, C., Kamei, K., Hara, S., and Inamori, Y. (1998) Cloning and nucleotide sequence of the gene encoding a serine proteinase inhibitor named marinostatin from a marine bacterium, *Alteromonas* sp. strain B-10−31, *Biosci. Biotechnol. Biochem. 62*, 2446−2449.
5. Carrell, R. W. (1988) Alzheimer's disease. Enter a protease inhibitor, *Nature 331*, 478−479.
6. Gebhard, W., and Hochstrasser, K. (1986) *Proteinase Inhibitors*, Elsevier, Amsterdam.
7. Laskowski, M., and Kato, I. (1980) Protein inhibitors of proteinases, *Annu. Rev. Biochem. 49*, 593−626.
8. Korsinczky, M. L., Schirra, H. J., Rosengren, K. J., West, J., Condie, B. A., Otvos, L., Anderson, M. A., and Craik, D. J. (2001) Solution structures by ^{1}H NMR of the novel cyclic trypsin inhibitor SFTI-1 from sunflower seeds and an acyclic permutant, *J. Mol. Biol. 311*, 579−591.
9. Bode, W., Papamokos, E., and Musil, D. (1987) The high-resolution X-ray crystal structure of the complex formed between subtilisin Carlsberg and eglin c, an elastase inhibitor from the leech Hirudo medicinalis. Structural analysis, subtilisin structure and interface geometry, *Eur. J. Biochem. 166*, 673−692.
10. Bode, W., and Huber, R. (1992) Natural protein proteinase inhibitors and their interaction with proteinases, *Eur. J. Biochem. 204*, 433−451.
11. Green, N. M., and Work, E. (1953) Pancreatic trypsin inhibitor, *Biochem. J. 54*, 347−352.
12. Rance, M., Sørensen, O. W., Bodenhausen, G., Wagner, G., Ernst, R. R., and Wüthrich, K. (1983) Improved spectral resolution in COSY proton NMR spectra of proteins via double quantum filtering, *Biochem. Biophys. Res. Commun. 117*, 479−485.
13. Bax, A., and Davis, D. G. (1985) MLEV-17-based two-dimensional homonuclear magnetization transfer spectroscopy, *J. Magn. Reson. 65*, 355−360.
14. Jeener, J., Meier, B. H., Bachmann, P., and Ernst, R. R. (1979) Investigation of exchange processes by two-dimensional NMR spectroscopy, *J. Chem. Phys. 71*, 4546−4553.
15. Billeter, M., Braun, W., and Wüthrich, K. (1982) Sequential resonance assignments in protein proton nuclear magnetic resonance spectra. Computation of sterically allowed proton-proton distances and statistical analysis of proton−proton distances in single-crystal protein conformations, *J. Mol. Biol. 155*, 321−346.
16. Wüthrich, K., Billeter, M., and Braun, W. (1983) Pseudostructures for the 20 common amino acids for use in studies of protein conformations by measurements of intramolecular proton-proton distance constraints with nuclear magnetic resonance, *J. Mol. Biol. 169*, 949−961.
17. Wüthrich, K., Billeter, M., and Braun, W. (1984) Polypeptide secondary structure determination by nuclear magnetic resonance spectra. Computation of sterically allowed proton-proton distances and statistical analysis of proton-proton distances in single crystal protein conformations, *J. Mol. Biol. 180*, 715−740.
18. Mer, G., Hietter, H., Kellenberger, C., Renatus, M., Luu, B., and Lefèvre, J.-F. (1996) Solution structure of PMP-C: A new fold in ht group of small serine proteinase inhibitors, *J. Mol. Biol. 258*, 158−171.
19. Wüthrich, K., Wider, G., Wagner, G., and Braun, W. (1982) Sequential resonance assignments as a basis for determination of spatial protein structures by high-resolution proton nuclear magnetic resonance, *J. Mol. Biol. 155*, 311−319.
20. Jackman, L. M., and Sternhell, S. (1969) *Applications of Nuclear Magnetic Resonance Spectroscopy in Organic Chemistry*, 2nd ed., Pergamon Press, Oxford.
21. Wishart, D. S., Sykes, B. D., and Richards, F. M. (1991) Relationship between nuclear magnetic resonance chemical shift and protein secondary structure, *J. Mol. Biol. 222*, 311−333.
22. Grathwohl, C., and Wüthrich, K. (1981) NMR studies of the rates of proline *cis-trans* isomerization in oligopeptides, *Biopolymers 20*, 2623−2633.
23. Brauer, A. B., Domingo, G. J., Cooke, R. M., Matthews, S. J., and Leatherbarrow, R. J. (2002) A conserved cis peptide bond is necessary for the activity of Bowman-Birk inhibitor protein, *Biochemistry 41*, 10608−10615.
24. Bai, Y., Milne, J. S., Mayne, L. M., and Englander, S. W. (1993) Primary structure effects on peptide group hydrogen exchange, *Proteins: Struct., Funct., Genet. 17*, 75−86.
25. McPhalen, C. A., Schnebli, H. P., and James, M. N. G. (1985) Crystal and molecular structure of the inhibitor eglin from

leeches in complex with subtilisin Carlsberg, *FEBS Lett. 188*, 55−58.
26. McPhalen, C. A., Svendsen, I., Jonassen, I., and James, M. N. G. (1985) Crystal and molecular structure of the inhibitor CI-2 from barley seeds in complex with subtilisin novo, *Proc. Natl. Acad. Sci. U.S.A. 82*, 7242−7246.
27. Heinz, D. W., Priestle, J. P., Rahuel, J., Wilson, K. S., and Grutter, M. G. (1991) Refined crystal structure of subtilisin novo in complex with wild-type and two mutant eglins, *J. Mol. Biol. 217*, 353−371.
28. Takeuchi, Y., Satow, Y., Nakamura, K. T., and Mitsui, Y. (1991) Refined crystal structure of the complex of subtilisin BPN′ and *Streptomyces* subtilisin inhibitor at 1.8 Å resolution, *J. Mol. Biol. 221*, 309−325.
29. Fujinaga, M., Sielecki, A., Read, R., Ardelt, W., Laskowski, M. J., and James, M. (1987) Crystal and molecular structures of the complex of alpha-chymotrypsin with its inhibitor turkey ovomucoid third domain at 1.8 Å resolution, *J. Mol. Biol. 195*, 397−418.
30. Hiromi, K., Akasaka, K., Mitsui, Y., Tonomura, B., and Murao, S. (1985) *Protein protease inhibitor—The case of Streptomyces subtilisin inhibitor (SSI)*, Elsevier, Amsterdam.

BI048034X